NASA CONTRACTOR REPORT

NASA CR-541

BUCKLING OF IMPERFECT CYLINDERS UNDER AXIAL COMPRESSION

by G. A. Thurston and M. A. Freeland

Prepared by
MARTIN-MARIETTA CORPORATION
Denver, Colo.
for Langley Research Center

NATIONAL AERONAUTICS AND SPACE ADMINISTRATION • WASHINGTON, D. C. • JULY 1966

NASA CR-541

BUCKLING OF IMPERFECT CYLINDERS UNDER AXIAL COMPRESSION

By G. A. Thurston and M. A. Freeland

Prepared under Contract No. NAS 1-4782 by
MARTIN-MARIETTA CORPORATION
Denver, Colo.

for Langley Research Center

NATIONAL AERONAUTICS AND SPACE ADMINISTRATION

For sale by the Clearinghouse for Federal Scientific and Technical Information
Springfield, Virginia 22151 – Price $3.00

CONTENTS

TABLES

FIGURES

BUCKLING OF IMPERFECT CYLINDERS

UNDER AXIAL COMPRESSION

By G. A. Thurston and M. A. Freeland
Martin-Marietta Corporation

SUMMARY

A solution is presented for Donnell's equations for an imperfect cylinder subjected to axial compression. Newton's method is used to reduce the nonlinear partial differential equations to a sequence of linearized equations. The linear equations are solved numerically by applying Galerkin's method.

Buckling loads are computed for several imperfection shapes, including the axisymmetric imperfections considered by Koiter. Some postbuckled solutions are also reported.

INTRODUCTION

Donnell's equations for an imperfect cylinder under axial compression are a pair of fourth order nonlinear partial differential equations. In this report, the solution of the nonlinear problem is reduced to solving a sequence of linear differential equations. The linear equations are derived by Newton's method or quasilinearization, as it is also known in the literature.

This direct solution of the governing differential equations is in contrast to the energy solutions for finite-deflection equations that have been reported in the past. From the theoretical standpoint, the two approaches reduce to a Galerkin solution compared to a Rayleigh-Ritz solution.

Newton's method has the practical advantage that it leads to a numerical solution of matrix arithmetic. The simple numerical manipulations make the solution easy to program for a digital computer. The present solution is programed to include up to 60 terms in the Fourier series solution for the normal displacement w and could be easily extended to more terms if desired. The maximum number of terms retained in a Rayleigh-Ritz solution has been reported as 15.

Among the first to treat the problem of the imperfect axially compressed cylinder were Donnell and Wan (ref. 1). Their work was based on Donnell's equations derived earlier (ref. 2). Although Donnell and Wan show great physical insight into the problem, their numerical results were computed on a desk calculator and, consequently, suffer from an insufficient number of free parameters in the energy solution. They also assumed that the imperfection shape is directly proportional to the deformed shape of the shell.

Subsequent investigations (refs. 3 and 4) have closely followed Donnell's method. With digital computers available, there seems to be no reason to assume proportionality between the shapes of the undeformed and deformed shell, and this restriction is dropped in the present analysis.

Donnell and Wan's approach follows closely the lines established by Von Kármán and Tsien (ref. 5) when they demonstrated the possibility that the cylinder is imperfection-sensitive. They showed the existence of equilibrium states at axial loads well below the classical buckling load. These postbuckled solutions of the finite-deflection equations for the perfect shell satisfy the pertinent compatibility equation exactly in terms of a deflection function represented by double Fourier series with undetermined coefficients. The coefficients then follow from minimizing the total potential energy. Hoff, Madsen, and Mayers (ref. 6) refer to this solution as the Von Kármán-Tsien-Leggett procedure and note that successive investigators (refs. 6 through 11) have used more and more terms in the Fourier series approximation as digital computers replaced desk calculators.

It seems appropriate to consider whether another type of solution is more suitable for programing on a digital computer. Newton's method leading to a Galerkin solution is offered here as an alternative.

The effect of boundary conditions on the prebuckled stress distribution in the axially compressed cylinder has received recent attention (refs. 12 through 14). The interaction between boundary conditions and imperfections would be a worthwhile topic for investigation. However, the effect of boundary conditions is neglected in the present analysis.

Koiter (refs. 15 and 16) demonstrates the reduction in buckling load caused by a single imperfection proportional to the axisymmetric buckling mode shape of the perfect shell. He uses it as an application of his general buckling theory (ref. 17). His upper bound solution is refined as a special case in the present report.

Hutchinson (ref. 18) has extended Koiter's analysis to include two parameters in the imperfection shape and also the effect of internal pressure. Some of his approximate results are checked in this report.

The one- and two-parameter solutions are valuable because they show analytically the relation between imperfections and buckling load. As the number of terms in the double Fourier series for the imperfection shape increases, it becomes more difficult to determine the effect of individual terms because of the nonlinear coupling between terms. A numerical solution is required, which is the subject of the current investigation.

SYMBOLS

a	mean radius of circular cylindrical shell
D	flexural rigidity, Eh^3/m^4
E	Young's modulus
F	Airy stress function
f_{ij}	Fourier coefficient in series for F
h	shell thickness
L	length of circular cylindrical shell
ℓ_x, ℓ_y	half-wave lengths in axial and radial direction, respectively
M	number of terms in truncated double Fourier series

$m^4 = 12(1 - \nu^2)$

N	number of waves in circumferential direction
N_x, N_y, N_{xy}	stress resultants
$\bar{N}_x$	average axial stress resultant, positive in compression
p	ratio of applied axial compression to classical buckling load for a perfect shell, $\left(\bar{N}_x m^2 a\right)/(2Eh^2)$
p_c	value of p at buckling
u, v, w	axial, circumferential, and radial displacements, respectively
U_b	bending strain energy
U_m	extensional strain energy
V	total potential energy
W	sum of Fourier coefficients in series for $w/h, \sum_{i=0}^{\infty} \sum_{j=0}^{\infty} w_{ij}(1 - \delta_{io})$
$\bar{W}$	sum of Fourier coefficients for imperfection shape, $\sum_{i=0}^{\infty} \sum_{j=0}^{\infty} \bar{w}_{ij}$
$\bar{w}$	radial imperfection from perfect circular cylinder

$\bar{w}_{ij}, w_{ij}$	Fourier coefficients in series for $\bar{w}$ and w, respectively
x,y	axial and circumferential coordinates on middle surface of shell, respectively
$\bar{x},\bar{y}$	nondimensional coordinates, $\bar{x} = (\mu x/a)$, $\bar{y} = (Ny/a)$
δ_{ij}	Kronecker delta
ϵ	average end shortening
$\epsilon_{c\ell}$	average end shortening in perfect shell at classical buckling load
$\epsilon_x, \epsilon_y, \epsilon_{xy}$	middle surface strains
μ	axial wave number
$\bar{\mu} = \frac{m}{2}\left(\frac{a}{h}\right)^{\frac{1}{2}}$	axial wave number for a buckling mode from linear theory
ν	Poisson's ratio ($\nu = 0.3$ in computed results)
∇^4	biharmonic operator, $(\partial^4/\partial x^4) + 2(\partial^4/\partial x^2 \partial y^2) + (\partial^4/\partial y^4)$
i,j,k,ℓ,m,n,r,s,t	running indices

THEORY

Donnell's Equations

Donnell's equations (ref. 2) for imperfect cylinders can be written

$$D\nabla^4 w - \frac{1}{a} F_{,xx} - L(F, w + \bar{w}) = 0 \tag{1a}$$

$$\nabla^4 F + \frac{Eh}{a} w_{,xx} + \frac{Eh}{2} L(w, w + 2\bar{w}) = 0 \tag{1b}$$

where the nonlinear operator L is defined by

$$L(S,T) = S_{,xx}T_{,yy} - 2S_{,xy}T_{,xy} + S_{,yy}T_{,xx} \tag{2}$$

and the commas in the subscripts denote repeated partial differentiation with respect to the independent variables following the comma.

Equation (1a) is the equilibrium equation summing forces on a differential element of the shell in the radial direction, see figure 1 for notation. The other two equilibrium equations consistent with Donnell's assumptions,

$$N_{x,x} + N_{xy,y} = 0 \tag{3a}$$

$$N_{xy,x} + N_{y,y} = 0 \tag{3b}$$

are satisfied identically by the Airy stress function F defined by

$$N_x = F_{,yy} \tag{4a}$$

$$N_y = F_{,xx} \tag{4b}$$

and

$$N_{xy} = - F_{,xy} \tag{4c}$$

Equation (1b) is the compatibility equation derived from the middle surface strain-displacement relations

$$\epsilon_x = u_{,x} + \frac{1}{2}\left(w_{,x} + 2\bar{w}_{,x}\right) w_{,x} \tag{5a}$$

$$\epsilon_y = v_{,y} - \frac{w}{a} + \frac{1}{2}\left(w_{,y} + 2\bar{w}_{,y}\right) w_{,y} \tag{5b}$$

$$\epsilon_{xy} = u_{,y} + v_{,x} + \frac{1}{2}\left(w_{,x} + 2\bar{w}_{,x}\right) w_{,y} + \frac{1}{2}\left(w_{,y} + 2\bar{w}_{,y}\right) w_{,x} \tag{5c}$$

and the stress-strain relations

$$\epsilon_x = \frac{1}{Eh}\left(F_{,yy} - \nu F_{,xx}\right) \tag{6a}$$

$$\epsilon_y = \frac{1}{Eh}\left(F_{,xx} - \nu F_{,yy}\right) \tag{6b}$$

$$\epsilon_{xy} = \frac{-2(1+\nu)}{Eh} F_{,xy} \tag{6c}$$

Newton's Method

The method of solution of the nonlinear equations, equations (1), is an extension (ref. 19) of Newton's method for finding roots of polynomials. The nonlinear terms in the differential equations are expanded in a Taylor's series about an approximate solution, and only linear terms are retained. This gives a linear system of differential equations for the correction to the current approximation.

Let (F_m, w_m) denote the m^{th} approximation to a solution of equations (1). The correction $(\delta F_m, \delta w_m)$ to this solution is defined by

$$F = F_m + \delta F_m \tag{7a}$$

$$w = w_m + \delta w_m \tag{7b}$$

Substituting equations (7) into equations (1) and neglecting nonlinear terms in δF_m and δw_m obtains

$$D\nabla^4(\delta w_m) - \frac{1}{a}(\delta F_m)_{,xx} - L(F_m, \delta w_m) - L(w_m + \bar{w}_m, \delta F_m) = -E_1 \tag{8a}$$

$$\nabla^4(\delta F_m) + \frac{Eh}{a}(\delta w_m)_{,xx} + Eh\, L(w_m + \bar{w}_m, \delta w_m) = -E_2 \tag{8b}$$

The right sides of equations (8) contain the errors in the current approximation to the solution of equations (1).

$$E_1 = D\,\nabla^4 w_m - \frac{1}{a} F_{m,xx} - L(F_m, w_m + \bar{w}) \tag{9a}$$

$$E_2 = \nabla^4 F_m + \left(\frac{Eh}{a}\right) w_{m,xx} + \frac{Eh}{2} L(w_m, w_m + 2\bar{w}) \tag{9b}$$

After solving equations (8), the iteration proceeds by replacing (F_m, w_m) in equations (7) with

$$F_{m+1} = F_m + \delta F_m \tag{10a}$$

$$w_{m+1} = w_m + \delta w_m \tag{10b}$$

and solving for $(\delta F_{m+1}, \delta w_{m+1})$, etc. If the correction $(\delta F_m, \delta w_m)$ approaches zero as m increases, the errors E_1 and E_2 will also approach zero, and the solution will converge to an exact solution of the nonlinear equations, equations (1).

Conversely, the error in the approximate solution can be small in some cases and Newton's method will not converge. The limiting case occurs when F and w are an exact solution and the variational equations, equations (8), become

$$D\,\nabla^4(\delta w) - \frac{1}{a}\delta F_{,xx} - L(F, \delta w) - L(w + \bar{w}, \delta F) = 0 \tag{11a}$$

$$\nabla^4(\delta F) + \left(\frac{Eh}{a}\right)\delta w_{,xx} + Eh\, L(w + \bar{w}, \delta w) = 0 \tag{11b}$$

If the homogeneous equations, equations (11), have a nontrivial solution, then a bifurcation point has been reached with an eigenvalue $p = p_c$ that defines a classical buckling load.

In approaching an eigenvalue $p = p_c$, using Newton's method, the solutions of equations (8) will contain a term of the form

$$\delta w_m = \frac{(\Delta p) w_c}{p_c^* - p} + \ldots \tag{12}$$

where $p_c^* \to p_c$ is the eigenvalue of equations (8), Δp is the load increment from the last convergent solution, and w_c is the component of the last solution equal to the eigenfunction associated with p_c^*. It can be seen that the load increment must be smaller and smaller for convergence as p approaches p_c.

Actually, equation (12) applies for snap buckling where $\frac{dp}{d\epsilon}$ vanishes. If the postbuckling mode is orthogonal to the prebuckling mode shape, equations (11) will apply, and there is no problem in applying Newton's method. A simple example of the latter case is the classical one of the bifurcation from an axisymmetric solution to an asymmetric one.

Recently, Bueckner, Johnson, and Moore (ref. 20) have shown how to modify Newton's method by changing variables for the case where $\frac{dp}{d\epsilon}$ vanishes. As yet, this modification has not been incorporated in the present computer program. The numerical approximation used in the program for the buckling loads is discussed in Appendix A.

Any method can be used to solve the linear partial differential equations, equations (8). The practical one adopted here is the Galerkin method, which leads to a numerical solution.

Numerical Solution

The analysis assumes initial imperfection shapes that can be represented by a double Fourier series

$$\bar{w} = h \sum_{i=0}^{\infty} \sum_{j=0}^{\infty} \bar{w}_{ij} \cos \frac{i\mu x}{a} \cos \frac{jNy}{a} \tag{13}$$

The solution is then sought in the form

$$w = w_m = h \sum_{i=0}^{\infty} \sum_{j=0}^{\infty} w_{ij} \cos \frac{i\mu x}{a} \cos \frac{jNy}{a} \tag{14a}$$

$$F = F_m = \frac{2Eah^2}{m^2} \left[- \frac{py^2}{2a^2} + \sum_{i=0}^{\infty} \sum_{i=0}^{\infty} f_{ij} \cos \frac{i\mu x}{a} \cos \frac{jNy}{a} \right] \tag{14b}$$

and

$$\delta F_m = \frac{2Eah^2}{m^2} \sum_{i=0}^{\infty} \sum_{j=0}^{\infty} \delta f_{ij} \cos \frac{i\mu x}{a} \cos \frac{jNy}{a} \tag{15a}$$

$$\delta w_m = h \sum_{i=0}^{\infty} \sum_{j=0}^{\infty} \delta w_{ij} \cos \frac{i\mu x}{a} \cos \frac{jNy}{a} \tag{15b}$$

Substituting equations (14) and equations (15) into equations (8), collecting terms, and equating the coefficients of

$$\cos i\bar{x} \cos j\bar{y} \qquad i=0,1,2,3,\ldots$$

$$j=0,1,2,3,\ldots$$

to zero leads to a doubly infinite set of linear algebraic equations for the Fourier coefficients δw_{ij} and δf_{ij}, (the current approximations for the coefficients w_{ij} and f_{ij} are known or assumed). Truncating the doubly infinite set of equations to allow for a finite number of coefficients is equivalent to a Galerkin solution of equations (8).

The differential operator L appearing in equations (8) will contain terms that are the product of trigonometric series. These can be rewritten using the identities

$$2 \cos A \cos B = \cos (A + B) + \cos (A - B)$$

$$2 \sin A \sin B = \cos (A - B) - \cos (A + B)$$

Therefore, if

$$S = \sum_{k=0}^{\infty} \sum_{\ell=0}^{\infty} S_{k\ell} \cos k\bar{x} \cos \ell\bar{y}$$

and

$$T = \sum_{m=0}^{\infty} \sum_{n=0}^{\infty} T_{mn} \cos m\bar{x} \cos n\bar{y}$$

then,

$$L(S,T) = \frac{\mu^2 N^2}{4a^4} L^*(S_{k\ell}, T_{mn}) = \frac{\mu^2 N^2}{4a^4} \sum_{k=0}^{\infty} \sum_{\ell=0}^{\infty} \sum_{m=0}^{\infty} \sum_{n=0}^{\infty} S_{k\ell} T_{mn} \Big\{ [\ell m - kn]^2 \cdot [\cos(k+m)\bar{x} \cos(\ell+n)\bar{y} + \cos(k-m)\bar{x} \cos(\ell-n)\bar{y}]$$

$$+ [\ell m + kn]^2 [\cos(k+m)\bar{x} \cos(\ell-n)\bar{y} + \cos(k-m)\bar{x} \cos(\ell+n)\bar{y}] \Big\} \quad (16)$$

It is tedious to rewrite the order of summation in the L^* operator to obtain the coefficients of $\cos i\bar{x} \cos j\bar{y}$. However, rather than writing these terms out explicitly, the computer solution is programed to pick up the correct coefficients from the L^* operator and insert them in the linear algebraic equations. This linearity in the matrix algebra means simplicity in programing and is the main advantage of Newton's method.

Details of the numerical solution are discussed in Appendix A.

Once the solution of the differential equations is obtained, other quantities of interest can be computed (see ref. 9 for example). The unit end shortening is

$$(\epsilon/\epsilon_{c\ell}) = p + \frac{m^4}{64} \left(\frac{\mu}{\bar{\mu}}\right)^2 \sum_{i=0}^{\infty} \sum_{j=0}^{\infty} i^2 w_{ij} (w_{ij} + 2\bar{w}_{ij}) (1 + \delta_{oj}) \quad (17)$$

The average normal deflection is determined by the coefficient w_{oo}, which does not appear in the algebraic equations but is determined from

$$w_{oo} = -\frac{2\nu p}{m^2} + \frac{m^2}{32}\left(\frac{N}{\bar{\mu}}\right)^2 \sum_{i=0}^{\infty}\sum_{j=0}^{\infty} j^2 w_{ij}(w_{ij} + 2\bar{w}_{ij})(1 + \delta_{io}) \tag{18}$$

The strain energy corresponding to membrane stresses is denoted by U_m

$$\frac{U_m}{ELah\,\pi}\frac{m^4}{8}\left(\frac{a}{h}\right)^2 = \frac{p^2}{2} + \frac{1}{8}\sum_{i=0}^{\infty}\sum_{j=0}^{\infty}\left(i^2\mu^2 + j^2N^2\right)^2 f_{ij}^2\,(1 + \delta_{io})(1 + \delta_{oj}) \tag{19}$$

The bending strain energy U_b is

$$\frac{U_b}{ELah\,\pi}\frac{m^4}{8}\left(\frac{a}{h}\right)^2 = \frac{1}{8}\left(\frac{h}{a}\right)^2 \sum_{i=0}^{\infty}\sum_{j=0}^{\infty}\left(i^2\mu^2 + j^2N^2\right)^2 w_{ij}^2\,(1 + \delta_{io})(1 + \delta_{oj}) \tag{20}$$

The total potential energy V is

$$V = V_m + V_b - \left[(ELah\,\pi)\frac{8}{m^4}\left(\frac{h}{a}\right)^2\right]\left[p(\epsilon/\epsilon_{c\ell})\right] \tag{21}$$

RESULTS

Axisymmetric Imperfection

Koiter (refs. 15 through 17) has demonstrated the reduction in buckling load caused by an axisymmetric imperfection,

$$\bar{w} = h\,\bar{w}_{20}\cos\frac{2\bar{\mu}x}{a} \tag{22}$$

of the same wavelength as the classical buckling mode. The axisymmetric solution is

$$w = \frac{ph}{1 - p} \bar{w}_{20} \cos \frac{2\bar{\mu}x}{a} \tag{23}$$

The criterion in the numerical solution for bifurcation into an asymmetric mode is the vanishing of the determinant of the algebraic equations derived in Appendix A, see equations (A12). Koiter obtains an upper bound for the critical load by setting the first coefficient on the trace of the determinant to zero. This coefficient is in the equation for terms coupled with $\cos \bar{\mu}x/a \cos Ny/a$.

Numerical results from a 48-term expansion are compared in figure 2 with Koiter's upper bound solution. The buckling loads are almost identical. Hutchinson's approximate formula is not bad for small imperfections (ref. 18).

Two-Term Imperfection

Hutchinson (ref. 18) assumed a two-term series for the imperfection shape

$$\bar{w} = h\bar{w}_{11} \cos \frac{\bar{\mu}x}{a} \cos \frac{\bar{\mu}y}{a} + h\, w_{20} \cos \frac{2\bar{\mu}x}{a} \tag{24}$$

in his study of pressurized cylinders under axial compression. As in the previous example, the wavelengths correspond to those of classical buckling modes.

Results from the present analysis are compared with Hutchinson's approximate solution in table 1. He neglects cubic terms that become important as the imperfections become larger; however, his paper shows analytically the coupling between the two imperfection terms. This coupling allows the individual deflection terms to grow faster than the well-known factor $p/(1 - p)$ that appears in equation (23) for the single-term imperfection.

Imperfections with Longer Wavelengths

Koiter and Hutchinson have shown that for a fixed amplitude those imperfections proportional to the buckling modes from linear theory produce the greatest reduction in buckling load. However, Donnell and Wan (ref. 1) argue that imperfection amplitudes in test specimens will vary with wavelength; the amplitude of the imperfections decreasing as the wavelengths get shorter. They introduce an "unevenness factor" U depending only on the fabrication process and assume an explicit relation that in our notation would be written

$$\bar{w}_{11} = \frac{Ua^2}{\left(h^2 \mu^{1.5} N^{0.5}\right)}$$

Since the wavelengths from linear theory are relatively short, it seemed worthwhile to study more general imperfections.

Imperfections proportional to the deformed shape of the shell in postbuckled unstable equilibrium positions were found to lower the buckling pressure for axisymmetric buckling of spherical caps (ref. 21). Guided by this prior experience, the next step was to find unstable equilibrium positions for the perfect cylinder.

Kempner's four-term expansion (ref. 9) at $p = 0.35$ furnished a first guess for the numerical iteration procedure. The number of terms in the numerical solution was increased in steps to the 48 terms shown in table 2. The table gives an example of the convergence of the double Fourier series as more and more terms are included. In this case, some of the later terms contribute to the third decimal place of the sum of the series. The slow convergence is a function of the longer wavelengths of the series. The leading term has an axial wavelength 9.25 times the checkerboard pattern $(\bar{\mu}/\mu = 9.25)$ of the buckling mode from linear theory and the number of waves in the circumferential direction is less also $(N/\bar{\mu} = 0.431)$.

On the other hand, 18 terms in the series are more than necessary to provide six significant figures in the sum of the series solution for the short wavelengths of the imperfections considered by Hutchinson.

The end shortening $\epsilon/\epsilon_{c\ell}$ listed in table 2 changes slowly with the increase in the number of terms.

Once the solution at $p = 0.35$ was known, it became an initial guess for solutions at neighboring values of p on the unstable load-end shortening curve shown in figure 3. For the perfect shell, the wave numbers μ and N are not known in advance for a given value of p, but are determined by a minimum of the total potential energy V defined in equation (21). Solutions of the differential equations were obtained for different combinations of μ and N, but the curve in figure 3 does not necessarily correspond to an exact minimum of the potential energy at all points. The potential energy for the solutions in figure 3 is plotted in figure 4. The minimum postbuckled load in figure 3 is $p = 0.1065$, which is comparable to Almroth's value (ref. 14) of $p = 0.108$.

The postbuckled solutions are discussed further in Appendix B.

The purpose of obtaining these solutions in the current study was to use them as imperfection shapes. Four shapes were selected from the postbuckled solutions for the perfect shell. They are defined in table 3. They are normalized so that the algebraic sum of the coefficients is unity, $\bar{W} = 1.0$. This defines an imperfection with a total amplitude approximately equal to the thickness of the cylinder.

Buckling loads were computed for shells of these four imperfection shapes with various values of $\bar{W}$, μ, and N to find the effect of varying amplitudes and wavelengths. The results are shown in figures 5 through 8.

The decrease in buckling loads from these imperfections is not as pronounced as the reduction for the same amplitude from the imperfections considered by Koiter (ref. 16) and Hutchinson (ref. 18). However, it appears that any imperfection shape with amplitude equal to the shell thickness will reduce the buckling load to approximately 50 percent of the classical value.

Comparison with Experiment

Most of the cylinders that have been fabricated and tested have been imperfect in shape. Only the new techniques, such as electroplating metal on a wax mandrel or spinning a plastic specimen inside of a cylindrical mandrel, have produced near perfect shells. Unfortunately, most experiments have not included a careful inspection to determine the exact shape of the test specimens.

Transducers now afford a rapid means of inspection through measuring changes of reluctance in the air gap between a pickup and the shell or measuring changes in inductance of a probe. The sensitivity of these methods must be improved before a complete check with theory will be possible.

The basic problem is related to the extremely short wavelengths that must be measured to check Koiter's contention that the most important Fourier coefficient in the imperfection shape is the one with the wavelength of the axisymmetric buckling mode for the perfect shell. As a typical example, consider the specimens tested by Babcock and Sechler (ref. 22).

Their specimens had nominal dimensions: $L = 10$ in., $a = 4.0$ in., and $h = 0.0045$ in. These dimensions give $\bar{\mu} = 26.95$, and classical theory predicts half wavelengths of $\ell_x = \ell_y = 0.465$ in. for the buckling mode $\cos(\bar{\mu}x/a) \cos(\bar{\mu}y/a)$. This is equivalent to $N = 27$ complete waves running around the circumference of the shell. For the axisymmetric mode, $\cos(2\bar{\mu}x/a)$, the axial half wavelength ℓ_x is 0.232 in.

The inspection data published by Babcock and Sechler (ref. 22) do not allow any accurate estimate of the amplitudes of imperfections in shape at these short wavelengths.

CONCLUSIONS

Newton's method has proved to be a practical means of increasing the number of terms in the Fourier series solution of Donnell's equations for imperfect cylinders.

The rate of convergence of this double Fourier series depends on the ratio of the wave numbers μ and N to the wave number $\bar{\mu}$ related to the linear buckling modes. As the wave numbers decrease below $\bar{\mu}$, the rate of convergence also decreases, and more terms M are needed in the series for an accurate solution.

The convergence of the series becomes part of the problem in trying to correlate theory and experiment for imperfect shells. In the series for the imperfection shape, the largest measured amplitudes are in terms with lower wave numbers while Koiter and Hutchinson have shown that even small terms at large wave numbers reduce the buckling load substantially.

This would imply that M should be a large number when studying actual test specimens.

The experimental problem of separating imperfections with high wave numbers from experimental "noise" adds to the overall problem.

The postbuckled equilibrium states of the axially compressed cylinder are of academic interest. Here, the proper theory seems to be the main question rather than any insurmountable difficulty in solving the final equations.

MARTIN-MARIETTA CORPORATION
MARTIN COMPANY
Denver, Colorado, March 15, 1966

APPENDIX A

COMPUTER SOLUTION

The formal solution of Donnell's equations using Newton's method reduces to two doubly infinite sets of algebraic equations for the unknown double Fourier series coefficients. The computer program is written to determine a finite number of these coefficients by writing a finite set of algebraic equations, solving the equations, and testing the solution vector for convergence in the iteration procedure of Newton's method.

The doubly infinite set of algebraic equations follow from setting coefficients of $\cos i\bar{x} \cos j\bar{y}$ to zero after combining equations (14) and (15) in equations (8)

$$\sum_{i=0}^{\infty}\sum_{j=0}^{\infty}\left\{\left[\left(i^2\mu^2 + j^2N^2\right)^2 \delta w_{ij} - \frac{2m^2a}{h}\, pi^2\mu^2\delta w_{ij} + \frac{2m^2a^2}{h^2}\, i^2\mu^2\delta f_{ij}\right]\right.$$

$$\left.[\cos i\bar{x} \cos j\bar{y}]\right\} - \frac{m^2a}{2h}\,\mu^2N^2\left[L^*\left(f_{k\ell},\ \delta w_{mn}\right) + L^*\left(w_{k\ell} + \bar{w}_{k\ell},\ \delta f_{mn}\right)\right] = E_{1}^{*} \quad \text{(A1)}$$

$$\sum_{i=0}^{\infty}\sum_{j=0}^{\infty}\left[\left(i^2\mu^2 + j^2N^2\right)^2 \delta f_{ij} - \frac{m^2i^2\mu^2}{2}\,\delta w_{ij}\right] \cos i\bar{x} \cos j\bar{y}$$

$$+ \frac{m^2h\mu^2N^2}{8a}\, L^*\left(w_{k\ell} + \bar{w}_{k\ell},\ \delta w_{mn}\right) = E_2^* \quad \text{(A2)}$$

where

$$E_1^* = \sum_{i=0}^{\infty}\sum_{j=0}^{\infty}\left\{\left[\left(i^2\mu^2 + j^2N^2\right)^2 w_{ij} - \frac{2m^2a}{h}\, pi^2\mu^2\left(w_{ij} + w_{ij} + \bar{w}_{ij}\right)\right.\right.$$

$$\left.\left. + \frac{2m^2a^2}{h^2}\, i^2\mu^2 f_{ij}\right]\left[\cos i\bar{x} \cos j\bar{x}\right]\right\} + \frac{m^2a}{2h}\,\mu^2N^2\, L^*\left(w_{k\ell} + \bar{w}_{k\ell},\ f_{mn}\right) \quad \text{(A3)}$$

$$E_2^* = -\sum_{i=0}^{\infty}\sum_{j=0}^{\infty}\left[\left(i^2\mu^2 + j^2N^2\right)^2 f_{ij} - \frac{m^2i^2\mu^2}{2}\, w_{ij}\right]\cos i\bar{x} \cos j\bar{y}$$

$$- \frac{m^2h}{16a}\,\mu^2N^2\, L^*\left(w_{k\ell} + 2\bar{w}_{k\ell},\ w_{mn}\right) \quad \text{(A4)}$$

APPENDIX A

Since the solution of Donnell's equations is sought in the form of two double Fourier series, the coefficients appear in the algebraic equations as doubly subscripted variables. However, in writing the FORTRAN computer program for a finite set of these coefficients, it became apparent that it is simpler to treat the coefficients as single subscripted variables. Each ij combination has a single subscript

$$ij = (ij)_r = i_r\, j_r \qquad r = 1,2,3....M \tag{A5}$$

The single r subscript is then used for each Fourier coefficient of that ij combination ($w_r = w_{ij}$, $f_r = f_{ij}$, etc, when $i = i_r$ and $j = j_r$).

With this notation, the L^* operator defined in equation (16) becomes the product of two sums each containing M terms. This product is found in the computer solution term by term. Only terms in L^* that correspond to one of the M combinations of ij are of interest in the Galerkin solution. The program searches the list of input for i_r and j_r and stores the subscripts for which

$$\begin{cases} i_r = i_s + i_t \\ j_r = j_s + j_t \end{cases} \quad \text{or} \quad \begin{cases} i_r = |i_s - i_t| \\ j_r = |j_s - j_t| \end{cases} \tag{A6}$$

and for which

$$\begin{cases} i_r = i_s + i_t \\ j_r = |j_s - j_t \end{cases} \quad \text{or} \quad \begin{cases} i_r = |i_s - i_t| \\ j_r = j_s + j_t \end{cases} \tag{A7}$$

It is a simple matter to equate the M coefficients to zero in each of equations (A1) and equations (A2), once it is known

from equations (A6) and equations (A7) that the s^{th} and t^{th} Fourier coefficients appear in the r^{th} equation.

The algebraic equations are programed in matrix notation. The equations are first written in extended form and then contracted to a single matrix equation. The extended form is

$$\left|\left(i_r^2\mu^2 + j_r^2N^2\right)^2 \delta w_r\right| - \frac{2m^2a}{h}\mu^2 p\left|i_r^2\delta w_r\right| + \frac{2m^2a^2}{h^2}\mu^2\left|i_r^2\delta f_r\right|$$

$$- \frac{m^2a}{2h}\mu^2N^2\left|\left|A\right|\right|\left|\delta f_r\right| - \frac{m^2a}{2h}\mu^2N^2\left|\left|B\right|\right|\left|\delta w_r\right| = \left|(E_1)_r\right| \qquad (A8)$$

$$\left|\left(i_r^2\mu^2 + j_r^2N^2\right)^2 \delta f_r\right| - \frac{m^2\mu^2}{2}\left|i_r^2\delta w_r\right|$$

$$+ \frac{m^2h}{8a}\mu^2N^2\left|\left|C\right|\right|\left|\delta w_r\right| = \left|(E_2)_r\right| \quad r = 1,2,\ldots M \qquad (A9)$$

The single vertical lines $\left|\ \right|$ denote column vectors and the double lines denote square matrices. In the above equations, matrix A equals matrix C; they are given separate names in the program to provide storage locations for the subsequent manipulations.

Each equation in the set is divided by $\left(i_r^2\mu^2 + j_r^2N^2\right)^2$ and the terms collected and stored in the form

$$-\left|\left|A^*\right|\right|\left|\delta f_r\right| + \left|\left|B^*\right|\right|\left|\delta w_r\right| = \left|(E_1^*)_r\right| \qquad (A10)$$

$$\left|\delta f_r\right| + \left|\left|C^*\right|\right|\left|\delta w_r\right| = \left|(E_2^*)_r\right| \qquad (A11)$$

Eliminating δf_r obtains

$$\left|\left|B^* + A^*C^*\right|\right|\left|\delta w_r\right| = \left|(E_1^*)_r\right| + \left|\left|A^*\right|\right|\left|(E_2^*)_r\right| \quad r = 1,2,\ldots M \qquad (A12)$$

APPENDIX A

The indicated matrix multiplications are performed along with the matrix inversion to solve for the δw_r. The δf_r follow from back substitution in equation (A11).

The aforementioned matrix algebra has been spelled out in detail to make a clearer comparison with the Von Kármán-Tsien-Leggett procedure. Mathematically, the Galerkin solution and Rayleigh-Ritz solution are equivalent. The Newton-Raphson iterative solution applied by Almroth (ref. 14) leads to almost the same linear equations as equations (A12). The difference is the amount of algebraic manipulation performed by the analyst compared to the amount done by the digital computer.

In the Von Kármán-Tsien-Leggett procedure, an equation equivalent to equations (A11) is written with the f_r and C^* set equal to zero. Then solving for δf_r, making $f_r = \delta f_r$, and substituting in the potential energy expression equation (21) and applying the minimization procedure lead to a set of nonlinear algebraic equations that are equivalent to setting the right side of equations (A12) equal to zero. Then, if the Newton-Raphson iterative procedure is used on the nonlinear algebraic equations, the result is equivalent to equations (A12). The difficulty is that, to differentiate the coefficients of the nonlinear algebraic equations in the application of the Newton-Raphson technique, the coefficients must be known explicitly in terms of the unknown Fourier coefficients w_{ij}.

In the procedure used here, Newton's method is applied directly to the Donnell differential equations and the matrix algebra is strictly a numerical operation to be performed by the computer program. This means that the number of terms M allowed in the Fourier series for w is limited only by computer storage and the numerical accuracy of the matrix subroutines.

The classical definition of a critical point where the homogeneous variational equations, equations (11), have a nonzero solution is approximated in the numerical solution by the vanishing of the determinant of the matrix, $||B^* + A^*C^*||$, in equations (A12) when the error vector on the right side is zero.

APPENDIX A

For snapthrough buckling, the critical point cannot be reached exactly and buckling loads p reported in the text are computed by using a Lagrange interpolation formula for p as a function of the determinate. Extrapolating to the point where the determinate is zero defines the critical value of p. For bifurcation buckling, the load can be varied to approach the zero determinant within any desired tolerance.

The best guess at a solution for starting the iteration procedure is a solution for a nearby set of parameters. The program stores the last solution obtained while new input data can be read to change p, μ, N, M, or any of the subscripted variables.

APPENDIX B

POSTBUCKLING SOLUTIONS

In studying postbuckled solutions for shallow spherical caps (refs. 19 and 21) under external pressure, it was found that a good assumed solution for starting the Newton's method iteration is the inverted shape that satisfies the nonlinear equations for the shell but not the boundary conditions. With this assumed solution, Newton's method converges to the stable postbuckled solution rather than the prebuckled solution or the unstable postbuckled solution.

It is natural to ask if a similar situation exists for the axially compressed cylinder. Is there a simple assumed solution that leads Newton's method to converge to a solution defining the postbuckled equilibrium configuration?

The solution that suggests itself is based on the deformed shell shape proposed by Yoshimura (ref. 23). This is a concave polyhedron formed by connecting plane triangles. Yoshimura derives the relations that must exist for the deformation to be inextensional. A repeating section of the deformed shell is sketched in plan-form in figure 10. The edges of the triangles are shown as dashed lines. The maximum deflections from the cylindrical shape, consistent with the Donnell approximations, are

$$d_1 = \frac{1}{3}\frac{a\pi^2}{2N^2} \text{ and } d_2 = \frac{2}{3}\frac{a\pi^2}{2N^2} \tag{B1}$$

where each circular cross-section has been deformed into an N-sided polygon.

Then, the deflected shape w in the first quadrant of the x-y coordinates is

$$\left.\begin{aligned} w &= \frac{a\pi^2}{2N^2}\left(-\frac{1}{3} + \frac{x}{\ell_x} - \frac{y^2}{\ell_y^2}\right) && \frac{y}{\ell_y} \le \frac{x}{\ell_x} \le 1 \\ &= \frac{a\pi^2}{2N^2}\left(-\frac{1}{3} - \frac{x}{\ell_x} + \frac{2y}{\ell_y} - \frac{y^2}{\ell_y^2}\right) && \frac{x}{\ell_x} \le \frac{y}{\ell_y} \le 1 \end{aligned}\right\} \tag{B2}$$

$$\ell_y = a\pi/N$$

APPENDIX B

The Fourier series expansion for this function is

$$w = \frac{a\pi^2}{12N^2} + \frac{a}{N^2}\sum_{i=1}^{\infty}\left(\frac{1}{2i^2}\cos\frac{2i\mu x}{a} - \frac{2}{i^2}\cos\frac{i\mu x}{a}\cos\frac{iNy}{a}\right) \qquad \text{(B3)}$$

This is a relatively simple expansion and seems to fit the need for an assumed solution. When equation (B3) is substituted into equation (A11) to find the coefficients of the stress function f_{ij} that make the error E_2 a minimum, the result is

$$f_{ij} = 0.$$

This result is not surprising since it merely states that the Fourier series expansion of this inextensional shape satisfies the compatibility equation.

The series equation (B3) and $f_{ij} = 0$ does <u>not</u> satisfy the equilibrium equation. Setting the first term in the vector E_1 in equation (A11) to zero gives an estimate for an assumed value of p in terms of the wave numbers. Several trial solutions were made following this scheme, but none converged. Another similar approach was tried using the expansion in equation (B3) perturbed by the multiplier $(1 + e)$ where e is a small constant. This gives a simple expression for the f_{ij} proportional to the assumed w_{ij}.

These trial solutions also did not converge.

Finally, a solution denoted as Case 7 by Hoff, et al. (ref. 6) was used as an assumed solution. The solution has 15 Fourier coefficients in the expansion for w. Seven have subscripts $i = j$ and six have $i = 2k$, $j = 0$, $k = 1,2,3,\ldots6$. This solution is for $p = 0.07$, which is lower than any value obtained for p by previous investigators. This solution was used as an assumed solution in the current computer program. The input data allowed for 49 terms in the expansion for w with the terms in addition to the first 15 assumed as zero.

APPENDIX B

This solution did not converge either. The lack of convergence was either due to the determinant of the algebraic equations, equations (A12), approaching zero near a critical load or because no solution exists at these values of p, μ, and N. The first iteration of the numerical solution showed that the 15-term solution of reference 6 contains errors from neglecting terms $j \neq i$ and $j \neq 0$ since the determinant was large but the correction vector for w was also relatively large in the previously neglected terms. Successive iterations appeared to converge until the sixth where the determinant almost vanished. Later iterations diverged.

The postbuckled deformation curve shown in figure 3 was obtained by first obtaining a solution at $p = 0.35$. The assumed solution for Newton's method was taken from Kempner's four-term expansion (ref. 9). The number of terms in the computer solution was gradually increased to 48. Once the solution at $p = 0.35$ was available, it was a simple matter to vary p using previous solutions as a first guess.

The lowest value of p on the postbuckled load-deflection curve in figure 3 is $p = 0.1065$. This is comparable to Almroth's lower buckling load of $p = 0.108$ obtained with 10 terms in the series for w. The solution at $p = 0.1065$ satisfies the differential equations but is not a minimum energy solution. The value of $N/\bar{\mu}$ was arbitrarily restricted to 0.288. The reason is that as p decreases, the value of N to achieve minimum potential energy also decreases. This leads to a conflict with Donnell's basic assumption that N is relatively large.

Since the purpose of the present investigation was to study the effect of initial imperfections on the upper buckling load, the question of the accuracy of Donnell's equations in the postbuckling range was not pursued. The solution obtained from the program at $p = 0.1067$, $\bar{\mu}/\mu = 15$, and $N/\bar{\mu} = 0.288$ is listed in table 4. It is compared with the coefficients of the Yoshimura shape defined by equation (B3). For the long wavelengths associated with this deflected shape, the terms in the Fourier series decrease slowly in magnitude, so that 48 terms is not a large number.

It appears that the proper value of the minimum postbuckling load is still an open question. It might be pointed out that the solutions of Donnell's equations could provide the first approximation to a solution of an improved theory by Newton's method.

REFERENCES

1. Donnell, L. H.; and Wan, C. C.: Effect of Imprefections on Buckling of Thin Cylinders and Columns under Axial Compression. J. Appl. Mech., vol. 17, 1950, pp. 73-83.

2. Donnell, L. H.: A New Theory for the Buckling of Thin Cylinders under Axial Compression and Bending. Trans. ASME, vol. 56, 1934, pp. 795-806.

3. Lu, S. Y.; and Nash, W. A.: Buckling of Initially Imperfect Axially Compressed Cylindrical Shells. Collected Papers on Instability of Shell Structures, NASA TN D-1510, 1962, pp. 187-202.

4. Lee, L. H. N.: Effects of Modes of Initial Imperfections on the Stability of Cylindrical Shells under Axial Compression. Collected Papers on Instability of Shell Structures, NASA TN D-1510, 1962, pp. 143-162.

5. von Karman, Th.; and Tsien, H. S.: The Buckling of Thin Cylindrical Shells under Axial Compression. J. Aeron. Sci., vol. 8, 1941, pp. 303-312.

6. Hoff, N. J.; Madsen, W. A.; and Mayers, J.: The Postbuckling Equilibrium of Axially Compressed Circular Cylindrical Shells. SUDAER No. 221, Stanford University Department of Aeronautics and Astronautics, Feb. 1965.

7. Leggett, D. M. A.; and Jones, R. P. N.: The Behavior of a Cylindrical Shell under Axial Compression When the Buckling Load has been Exceeded. Aeronautical Research Council Reports and Memoranda No. 2190, Aug. 1942.

8. Michielsen, H. F.: The Behavior of Thin Cylindrical Shells after Buckling under Axial Compression. J. Aeron. Sci., vol. 15, 1948, pp. 738-744.

9. Kempner, J.: Postbuckling Behavior of Axially Compressed Cylindrical Shells. J. Aeron. Sci., vol. 17, 1954, pp. 329-342.

10. Thielemann, W.: New Developments in the Nonlinear Theories of Buckling of Thin Cylindrical Shells. Proceedings of the Durand Centennial Conference, Pergamon Press, Inc., New York, 1960, pp. 76-119.

11. Almroth, B. O.: Postbuckling Behavior of Axially Compressed Circular Cylinders. AIAA J., vol. 1, Mar. 1963, pp. 630-633.

12. Stein, M.: The Effect on the Buckling of Perfect Cylinders of Prebuckling Deformations and Stresses Induced by Edge Support. Collected Papers on Instability of Shell Structures, NASA TN D-1510, 1962, pp. 217-227.

13. Fischer, G.: Über den Einfluss der gelenkigen Lagerung auf die Stabilitat dunnwandiger Kreiszylinderschalen unter Axiallast and Innendruck. Z. Flugwissenschaften, vol. 11, 1963, pp. 111-119.

14. Almroth, B. O.: Influence of Edge Conditions on the Stability of Axially Compressed Cylindrical Shells. NASA CR-161, Feb. 1963.

15. Koiter, W. T.: The Effect of Axisymmetric Imperfections on the Buckling of Cylindrical Shells Under Axial Compression. 6-90-63-86, Lockheed Missiles and Space Company, Sunnyvale, California, Aug. 1963.

16. Koiter, W. T.: Elastic Stability and Postbuckling Behavior. Proceedings, Symposium Nonlinear Problems, (R. E. Langer, ed.) University of Wisconsin Press, Madison, Wisconsin, 1963, pp. 257-275.

17. Koiter, W. T.: On the Stability of Elastic Equilibrium. Ph.D. Thesis, Delft, H. J. Paris, Amsterdam, 1945.

18. Hutchinson, J.: Axial Buckling of Pressurized Imperfect Cylindrical Shells. AIAA J., vol. 3, Aug. 1965, pp. 1461-1466.

19. Thurston, G. A.: Newton's Method Applied to Problems in Nonlinear Mechanics. J. Appl. Mech., vol. 32, June 1965, pp. 383-388.

20. Bueckner, H. F.; Johnson, M. W., Jr.; and Moore, R. H.: The Calculation of Equilibrium States of Elastic Bodies by Newton's Method. Technical Report No. 565, U. S. Army Mathematics Research Center, University of Wisconsin, Madison, Wisconsin, June 1965 (Also presented at 9th Midwestern Mechanics Conference, Madison, Wisconsin, Aug. 1965).

21. Thurston, G. A.: Comparison of Experimental and Theoretical Buckling Pressure for Spherical Caps. Collected Papers on Instability of Shell Structures, NASA TN D-1510, 1962, pp. 515-521.

22. Babcock, C. D. and Sechler, E. E.: The Effect of Initial Imperfections on the Buckling Stress of Cylindrical Shells. NASA TN D-2005, July 1963.

23. Yoshimura, Y.: On the Mechanism of Buckling of a Circular Cylindrical Shell under Axial Compression. NACA TM 1390, July 1955.

TABLE 1

TWO-PARAMETER IMPERFECTION WITH SHORT WAVELENGTHS

($\bar{\mu}/\mu = 1.0 \quad N/\bar{\mu} = 1.0$)

Imperfection coefficients		Buckling load, p_c	
$\bar{w}_{20}$	$\bar{w}_{11}$	Hutchinson (ref. 18)	Present analysis
.04	.0	.70	.83
.0	.06	.70	.72
.012	-.04	.70	.707
.0	.2	.50	.55
.017	-.167	.50	.53
.047	-.095	.50	.54
.145	-.145	.30	.465

Magnification factors from finite deflection theory

Imperfection coefficients		Load	Linear factor	Nonlinear	
$\bar{w}_{20}$	$\bar{w}_{11}$	p	$\frac{p}{1-p}$	$w_{20}/\bar{w}_{20}$	$w_{11}/\bar{w}_{11}$
.017	-.167	.45	.818	1.970	1.119
		.50	1.000	3.175	1.642
		.52	1.083	4.480	2.176
.047	-.095	.45	.818	1.002	1.409
		.50	1.000	1.369	2.103
		.52	1.083	1.638	2.664
.145	-.145	.30	.429	.491	1.095
		.35	.539	.669	1.745
		.40	.667	1.075	3.563

TABLE 2

CONVERGENCE OF SERIES FOR POSTBUCKLED SOLUTION FOR PERFECT SHELL

($p = 0.35$; $\bar{\mu}/\mu = 9.25$; $N/\bar{\mu} = 0.431$)

			Kempner (ref. 9)	Number of terms in present analysis			
				8	15	24	48
w_{oo}			.78	.4011	.1883	.0964	.0374
$\epsilon/\epsilon_{c\ell}$			.6	.4122	.3936	.3851	.3810
W			7.7	7.1169	6.0868	5.3372	4.7206
Fourier subscripts			w_{ij}	w_{ij}	w_{ij}	w_{ij}	w_{ij}
r	i	j		8-terms	15-terms	24-terms	48-terms
1	1	1	6.67	4.593	3.1556	2.4122	1.8749
2	2	2	0	.625	.5834	.4892	.3810
3	1	3	0	.047	.0851	.0882	.0720
4	3	1	0	.711	.5764	.4367	.3202
5	2	0	.667	.613	.3642	.2409	.1544
6	0	2	.334	.355	.2797	.2214	.1633
7	4	0		.174	.1829	.1401	.0964
8	0	4		-.00083	.0031	.0056	.0049
9	3	3			.0662	.0808	.0739
10	2	4			.0023	.0081	.0085
11	1	5			-.0011	-.0013	-.0024
12	0	6			-.000096	-.00028	-.0007
13	6	0			.0951	.1026	.0807
14	5	1			.2941	.2653	.2044
15	4	2			.3998	.3764	.3162
16	4	4				.0031	.0056
17	3	5				-.0013	-.0025
18	2	6				-.0005	-.0014
19	1	7				-.000075	-.0003
20	0	8				-.0000021	-.000014
21	8	0				.0615	.0663
22	7	1				.1610	.1502
23	6	2				.1928	.1860
24	5	3				.0548	.0635

TABLE 2. - CONCLUDED

Fourier Subscripts			Kempner (ref. 9) w_{ij}	Number of terms in present analysis			
				8 w_{ij} 8-terms	15 w_{ij} 15-terms	24 w_{ij} 24-terms	48 w_{ij} 48-terms
r	i	j					
25	5	5					-.0024
26	4	6					-.0012
27	3	7					-.00027
28	2	8					-.000026
29	1	9					.0000041
30	0	10					.0000010
31	10	0					.0511
32	9	1					.1109
33	8	2					.1113
34	7	3					.0430
35	6	4					.0023
36	6	6					-.00087
37	5	7					-.00021
38	4	8					-.000024
39	3	9					.0000032
40	2	10					.0000019
41	1	11					.00000037
42	0	12					.000000017
43	12	0					.0321
44	11	1					.0745
45	10	2					.0646
46	9	3					.0228
47	8	4					-.00035
48	7	5					-.0021

TABLE 3

IMPERFECTION SHAPES FROM SOLUTION ON UNSTABLE BRANCH OF PERFECT CYLINDER

			Shape I	Shape II	Shape III	Shape IV
Parameters in perfect shell solution						
p			.30	.40	.5	.6
$\bar{\mu}/\mu$			20.	17.5	10.	10.
$N/\bar{\mu}$			.288	.288	.288	.288
W			9.528	6.521	3.216	2.594
r	i	j	Normalized mode shapes $\bar{W} = 1$			
			$\bar{w}_{ij}$	$\bar{w}_{ij}$	$\bar{w}_{ij}$	$\bar{w}_{ij}$
1	1	1	.352	.305	.1257	.112
2	2	2	.0938	.1165	.1636	.179
3	1	3	-.0219	.0291	.0539	.050
4	3	1	.0594	.0467	.0327	.0276
5	2	0	.0293	.0217	.0156	.0130
6	0	2	.0384	.0435	.0655	.0595
7	4	0	.0195	.0160	.00138	.0120
8	0	4	.0302	.00524	.00116	.0113
9	3	1	.0238	.0333	.0701	.0745
10	2	4	.00568	.0103	.0235	.023
11	1	5	.000754	.00298	.00099	.0103
12	0	6	-.00011	.000234	.00018	.0021
13	6	0	.0157	.0130	.01111	.0097
14	5	1	.0376	.0306	.0255	.0223
15	4	2	.0727	.0740	.0472	.0450
16	4	4	.00481	.00944	.0245	.0256
17	3	5	.00052	.00254	.00948	.0101
18	2	6	-.00023	.000388	.00343	.0044
19	1	7	-.00014	0	0	.0012
20	0	8	0	0	0	0
21	8	0	.0119	.0100	.00942	.0087
22	7	1	.0268	.0228	.0211	.0193
23	6	2	.0396	.0375	.0285	.0270
24	5	3	.0229	.0331	.0504	.0575

TABLE 3. - CONLCUDED

			Shape I	Shape II	Shape III	Shape IV
Parameters in perfect shell solution						
			Normalized mode shapes $\bar{W} = 1$			
r	i	j	$\bar{w}_{ij}$	$\bar{w}_{ij}$	$\bar{w}_{ij}$	$\bar{w}_{ij}$
25	5	5	.00022	.00186	.00796	.0087
26	4	6	-.00023	.00241	.00271	.0032
27	3	7	-.00012	0	0	0
28	2	8	0	0	0	0
29	1	9	0	0	0	0
30	0	10	0	0	0	0
31	10	0	.00856	.0074	.00755	.0075
32	9	1	.0194	.0170	.0169	.0163
33	8	2	.0242	.0233	.0206	.0205
34	7	3	.01824	.0260	.0299	.0336
35	6	4	.00369	.0081	.0208	.0233
36	6	6	-.00019	0	.00171	.0021
37	5	7	0	0	0	0
38	4	8	0	0	0	0
39	3	9	0	0	0	0
40	2	10	0	0	0	0
41	1	11	0	0	0	0
42	0	12	0	0	0	0
43	12	0	.00543	.00505	.00574	.0062
44	11	1	.0130	.012	.0129	.0133
45	10	2	.0149	.0149	.0151	.0157
46	9	3	.0118	.0165	.0183	.0207
47	8	4	.00236	.00565	.0139	.0162
48	7	5	0	.00112	.00558	.0064

TABLE 4

POSTBUCKLED SOLUTIONS

		Yoshimura (ref. 23) inextensional shape	Hoff et al. (ref. 6)	Present analysis		
p		-	.0707	.12	.12	.1067
$\bar{\mu}/\mu$		-	42.7	15.	15.	15.
N/μ		-	.118	.288	.288	.288
$\epsilon/\epsilon_{c\ell}$		-	5.62	1.110	.582	.823
W		-	236.	33.4	27.2	29.8
i	j	$w_{ij}N^2h/a$	$w_{ij}N^2h/a$	$w_{ij}N^2h/a$	$w_{ij}N^2h/a$	$w_{ij}N^2h/a$
0	0	.823	.685	.3010	.1383	.2208
1	1	2.0	2.060	1.4779	1.0047	1.2819
2	2	-.5	-.466	-.1172	.0339	-.0506
1	3	0	.02790	.0204	-.0415	-.0190
3	1	0	-.0625	.2438	.1972	.2280
2	0	.5	.511	.4067	.1951	.3013
0	2	0	0	-.0872	.0028	-.0438
4	0	.125	.0866	.1558	.0884	.0215
0	4	0	0	.0049	.0045	.0102
3	3	.222	.1580	.0084	-.0360	-.0202
2	4	0	0	.0097	.0083	.0191
1	5	0	0	-.0094	.0058	-.0047
0	6	0	0	.0016	-.0011	-.0010
6	0	.05555	.02800	.0783	.0529	.0063
5	1	0	0	.0914	.0967	.0998
4	2	0	0	-.0615	.0197	-.0250
4	4	-.1250	-.0681	.0087	.0070	.0162
3	5	0	0	-.0085	.0052	-.0045
2	6	0	0	.0031	-.0021	-.0018
1	7	0	0	.00001	-.0007	.0014
0	8	0	0	-.0002	.0002	-.00009
8	0	.03125	.00894	.0407	.0317	.0371
7	1	0	0	.0374	.0507	.0473
6	2	0	0	-.0399	-.0019	-.0251
5	3	0	0	.0052	-.0299	-.0168

TABLE 4. - CONCLUDED

		Yoshimura (ref. 23) inextensional shape	Hoff et al. (ref. 6)	Present analysis		
i	j	$w_{ij}N^2h/a$	$w_{ij}N^2h/a$	$w_{ij}N^2h/a$	$w_{ij}N^2h/a$	$w_{ij}N^2h/a$
5	5	.08	.02880	-.0071	.0042	-.0042
4	6	0	0	.0029	-.0020	-.0014
3	7	0	0	-.00005	-.0006	.0013
2	8	0	0	-.0005	.0004	-.0002
1	9	0	0	.0002	.00003	-.0001
0	10	0	0	-.00002	-.00002	.00003
10	0	.0200	.00223	.0201	.0180	.0197
9	1	0	0	.0126	.0256	.0205
8	2	0	0	-.0266	-.0092	-.0214
7	3	0	0	.0061	-.0199	-.0084
6	4	0	0	.0063	.0066	.0129
6	6	-.0556	-.01225	.0025	-.0018	-.0009
5	7	0	0	-.0002	-.0004	.0011
4	8	0	0	-.0004	.0003	-.0002
3	9	0	0	.0002	.00003	-.0001
2	10	0	0	-.00004	-.00004	.00005
1	11	0	0	-.000005	.000002	-.000004
0	12	0	0	.000003	.000002	-.000002
12	0	.01388	.00037	.0085	.0081	.0086
11	1	0	0	.0044	.0122	.0089
10	2	0	0	-.0166	-.0090	-.0149
9	3	0	0	.0068	-.0114	0.0022
8	4	0	0	.0035	.0065	.0096
7	5	0	0	-.0054	.0029	-.0038

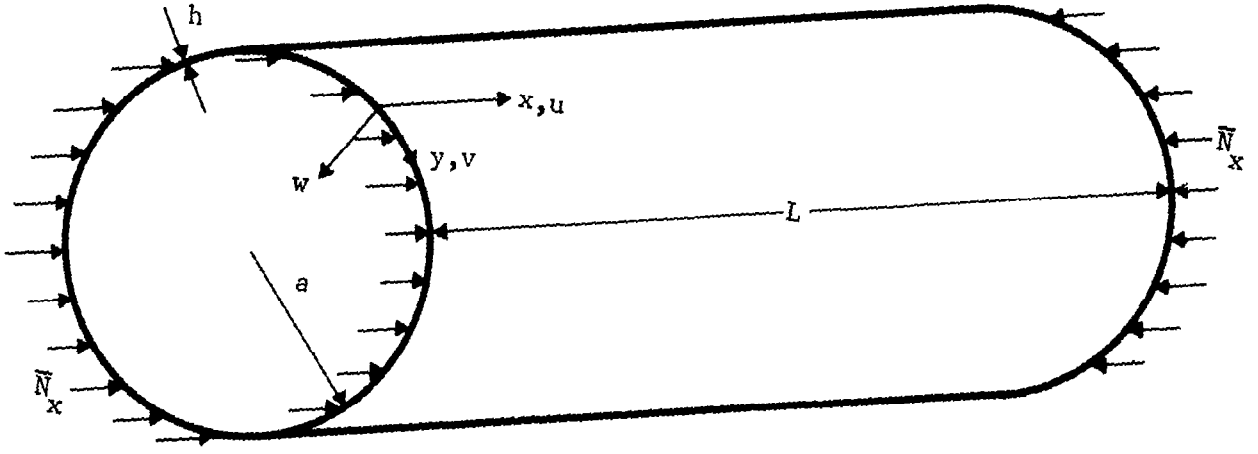

FIGURE 1. -- NOTATION FOR COORDINATES AND COMPONENTS OF DISPLACEMENTS OF AXIALLY COMPRESSED CYLINDER

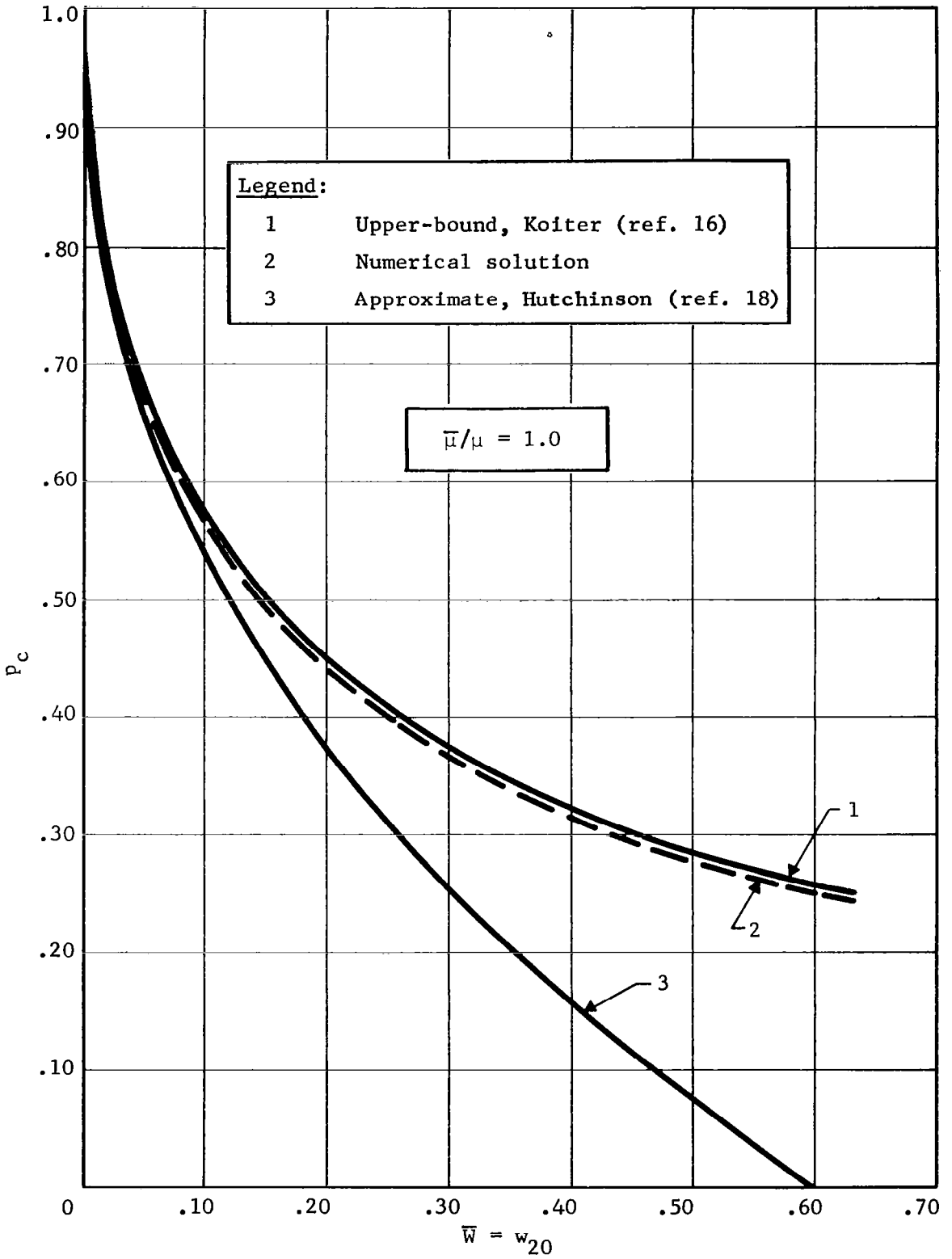

FIGURE 2. -- EFFECT OF AXISYMMETRIC IMPERFECTION ON AXIAL BUCKLING LOAD

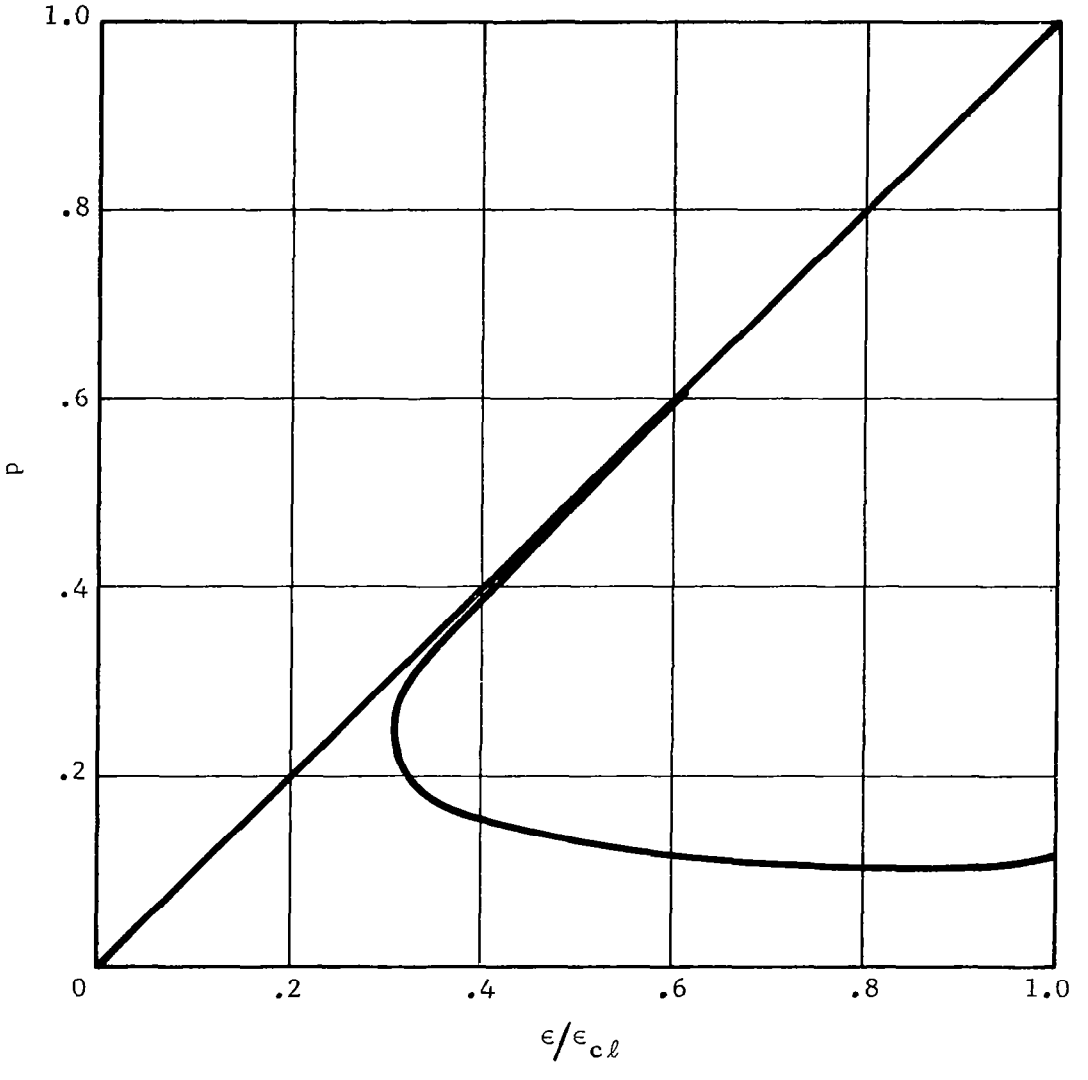

FIGURE 3. -- LOAD-END SHORTENING CURVES FOR PERFECT SHELL

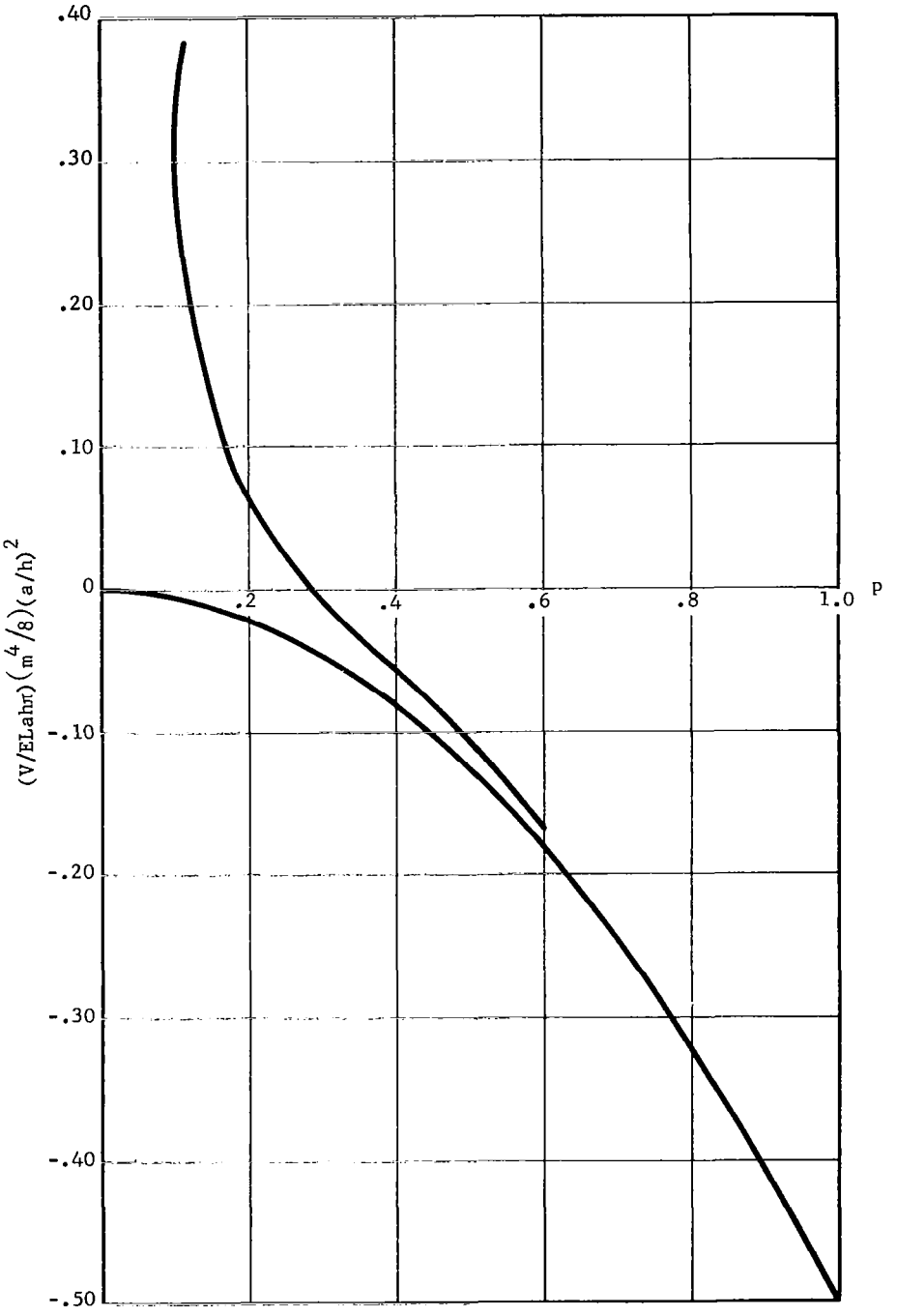

FIGURE 4. -- TOTAL POTENTIAL ENERGY VS LOAD FOR PERFECT SHELL

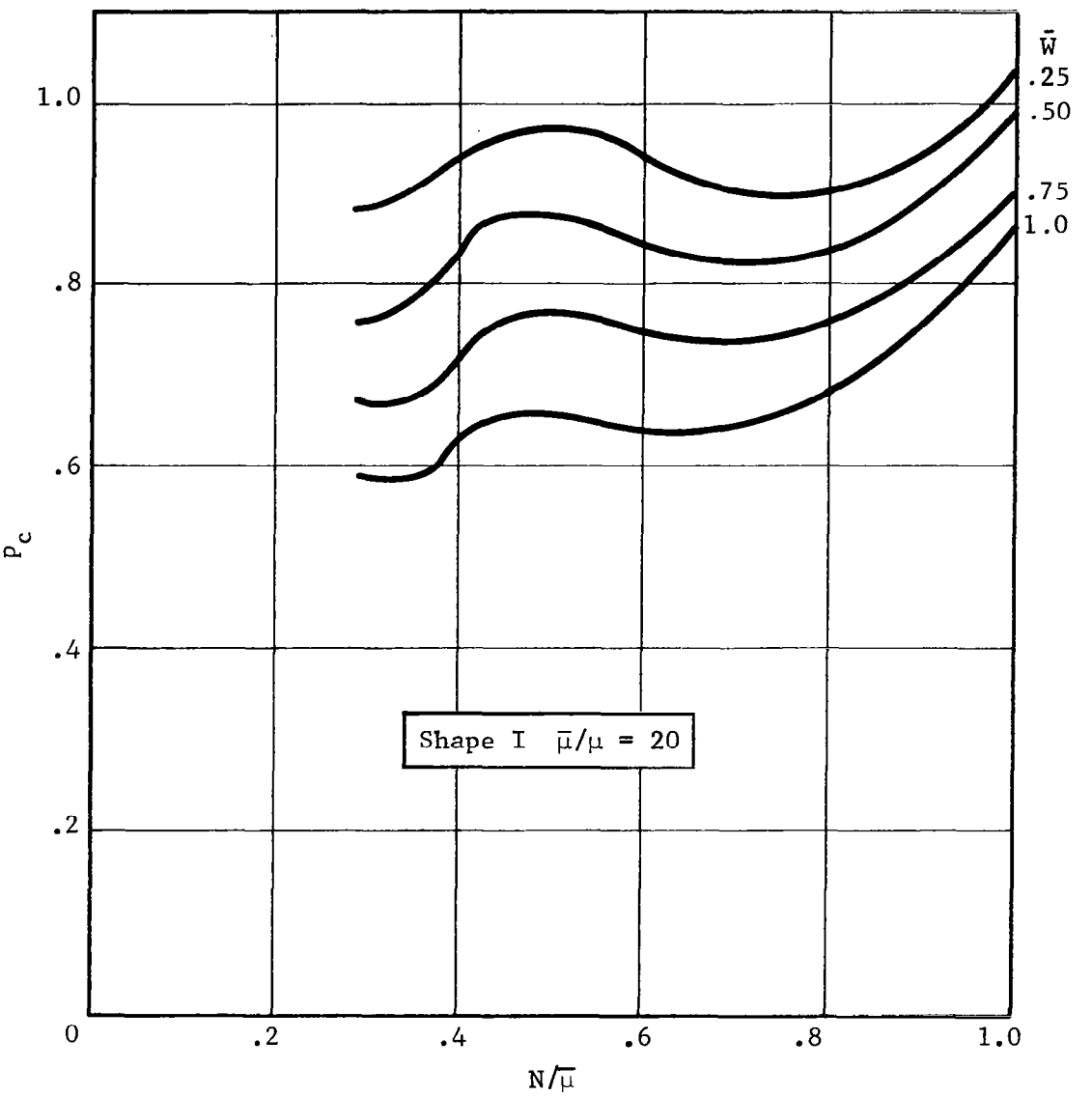

FIGURE 5. -- BUCKLING LOAD VS CIRCUMFERENTIAL WAVE NUMBER FOR VARIOUS IMPERFECTION AMPLITUDES

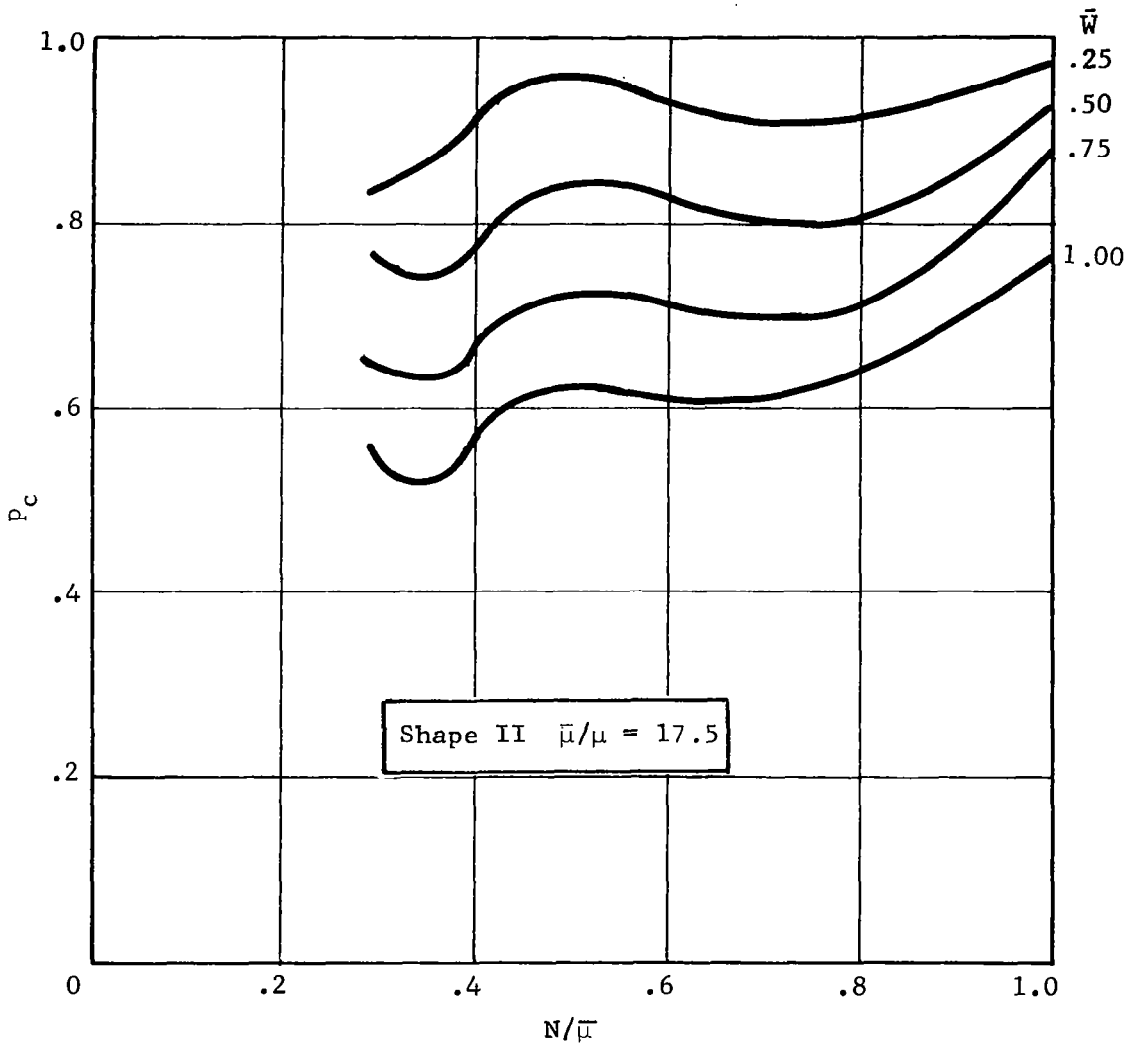

FIGURE 6. -- BUCKLING LOAD VS CIRCUMFERENTIAL WAVE NUMBER FOR VARIOUS IMPERFECTION AMPLITUDES

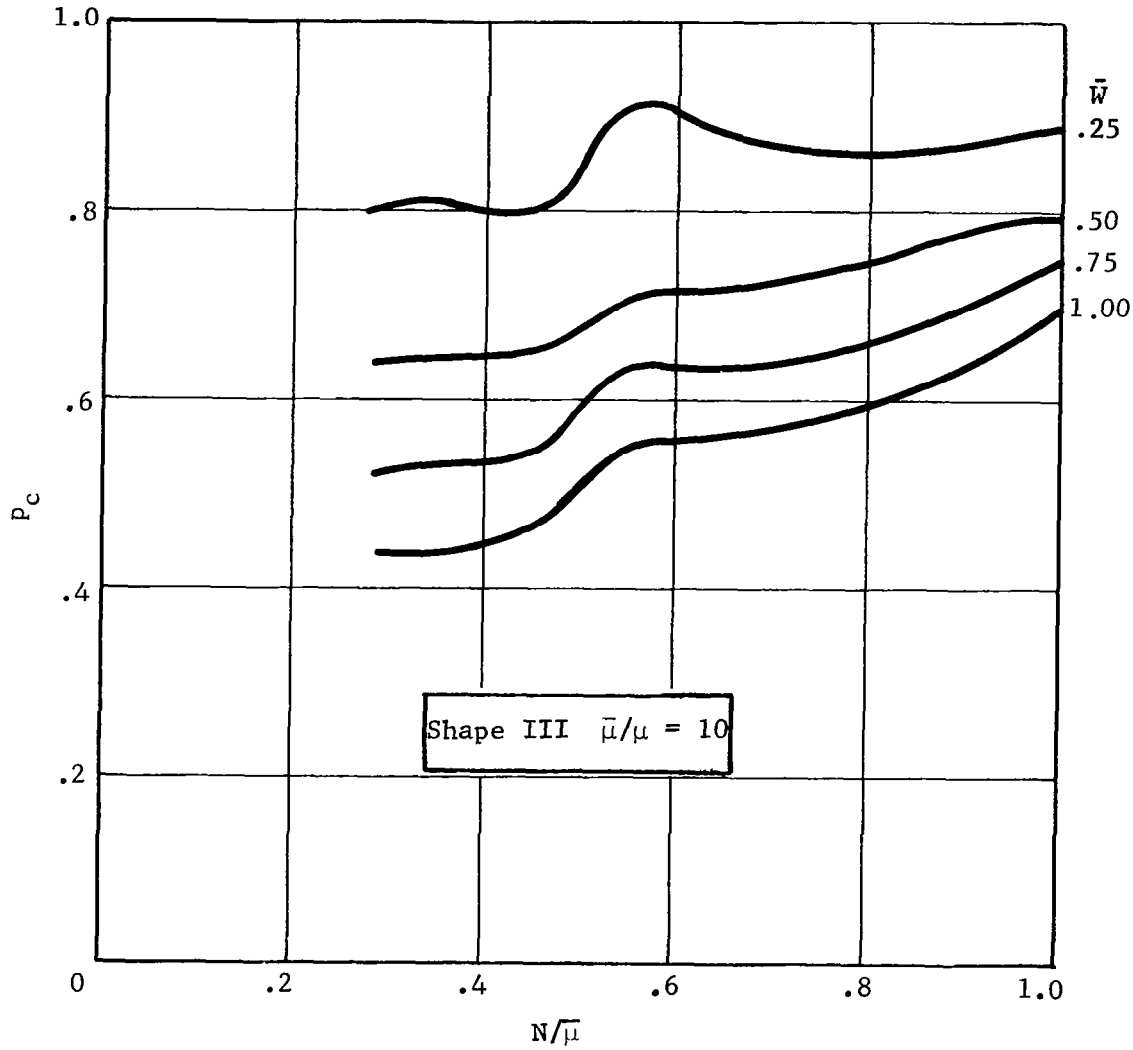

FIGURE 7. -- BUCKLING LOAD VS CIRCUMFERENTIAL WAVE NUMBER FOR VARIOUS IMPERFECTION AMPLITUDES

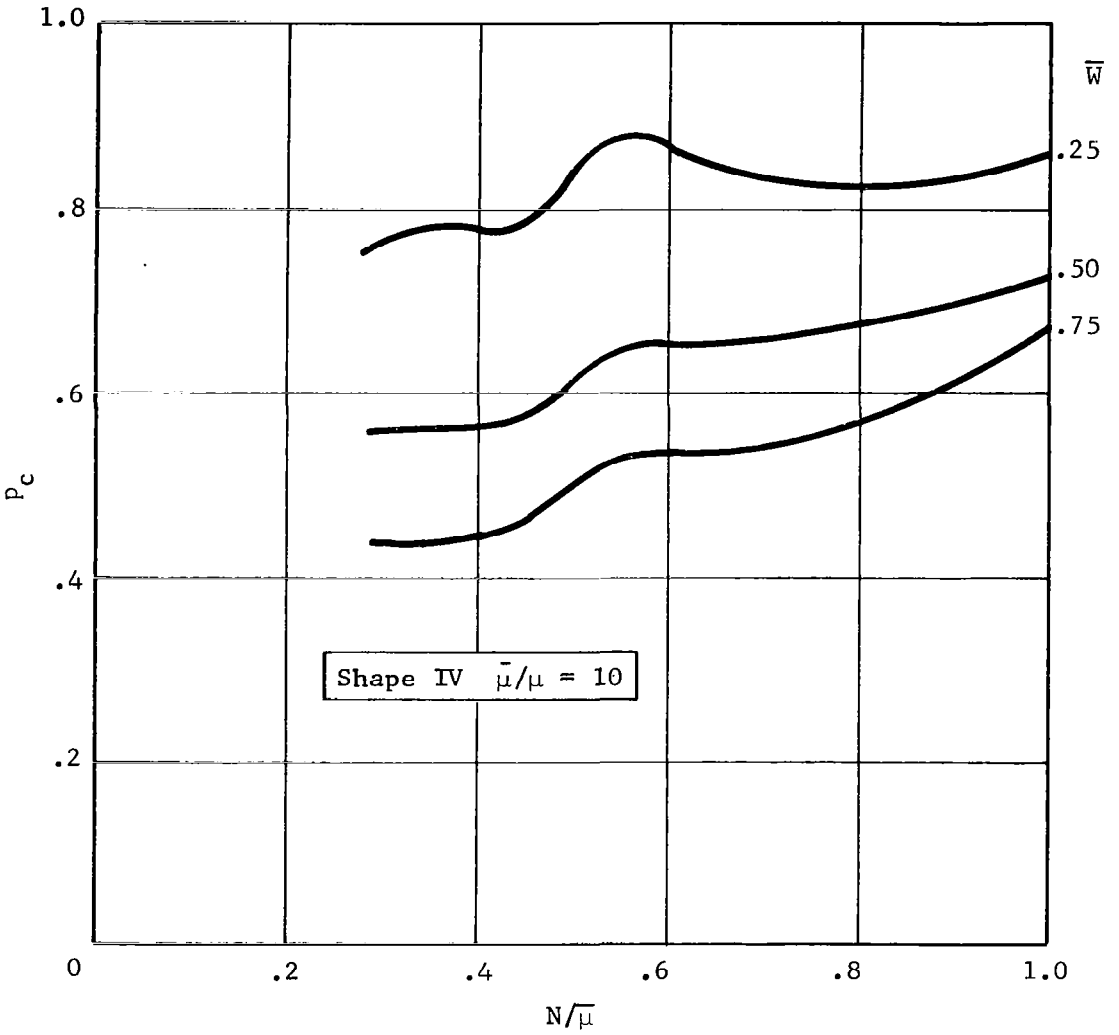

FIGURE 8. -- BUCKLING LOAD VS CIRCUMFERENTIAL WAVE NUMBER FOR VARIOUS IMPERFECTION AMPLITUDES

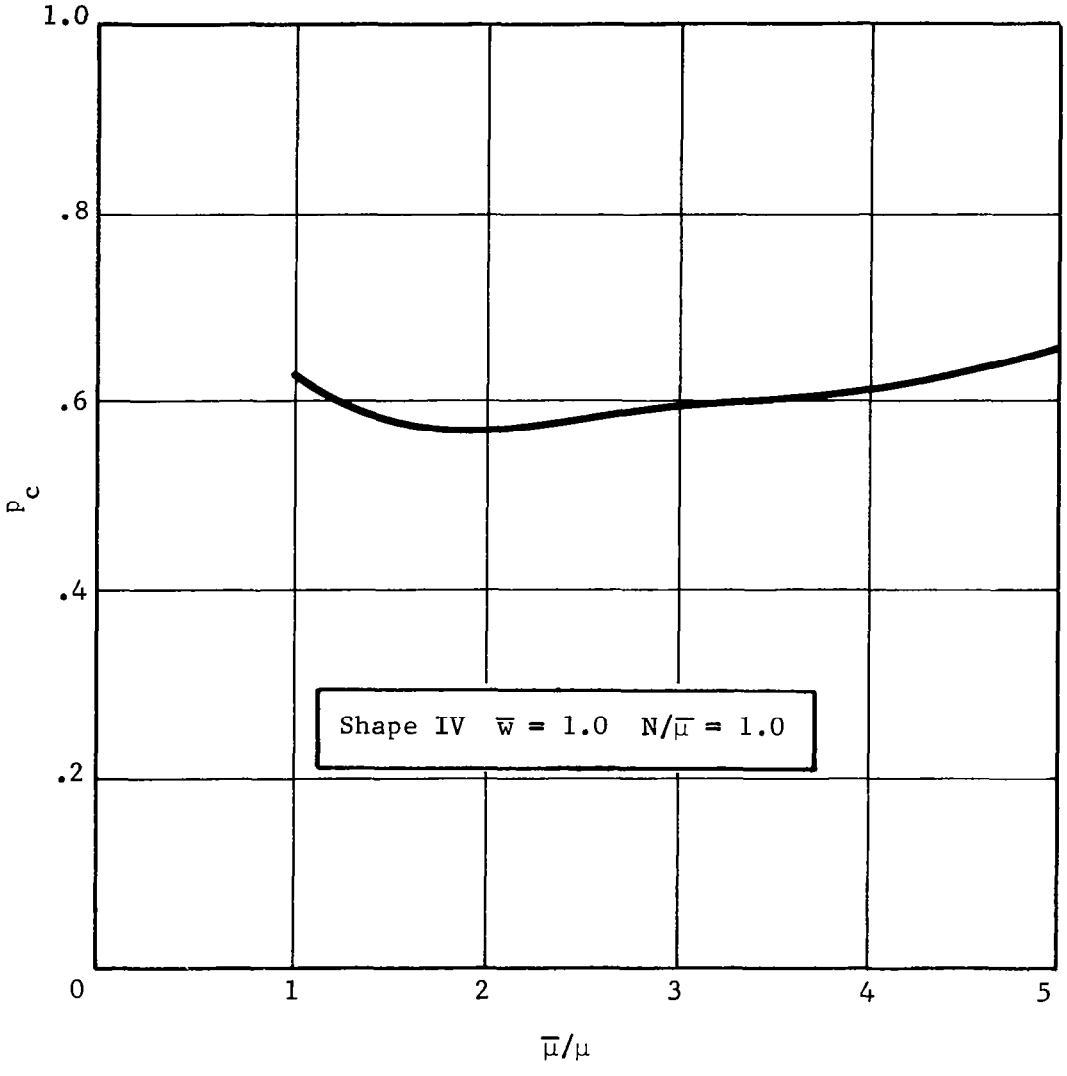

FIGURE 9. -- BUCKLING LOAD VS RATIO OF AXIAL WAVE NUMBERS FOR GIVEN IMPERFECTION

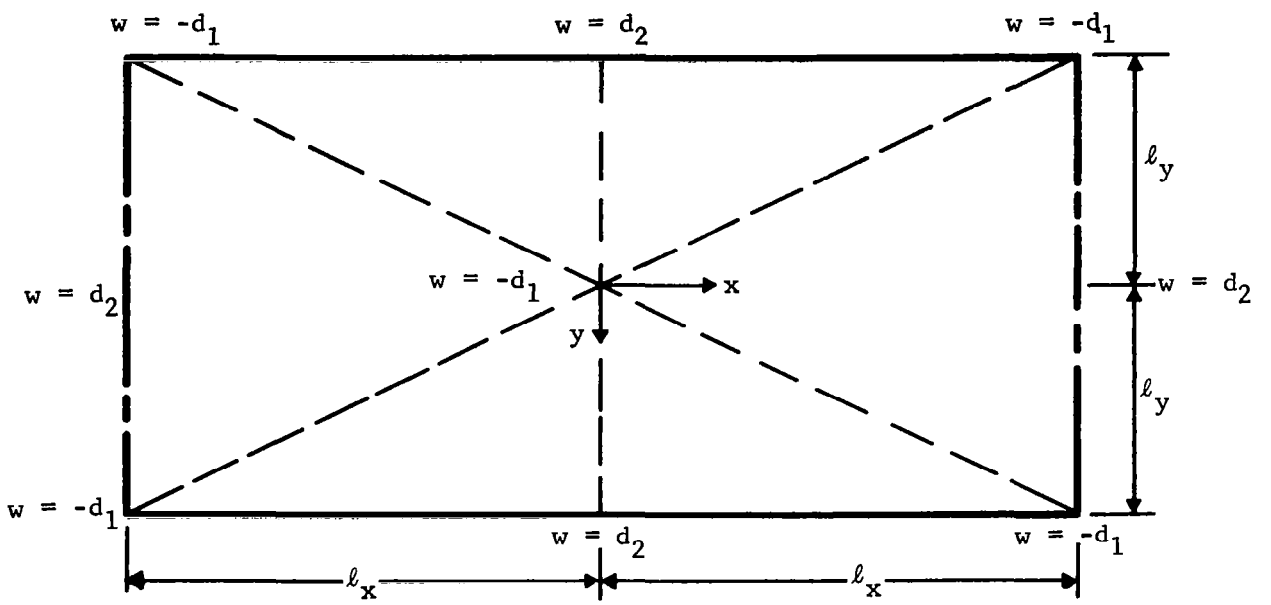

$$d_1 = \frac{1}{3}\frac{a\pi^2}{2N^2} \qquad d_2 = \frac{2}{3}\frac{a\pi^2}{2N^2} \qquad \ell_y = \frac{a\pi}{N}$$

FIGURE 10. -- NOTATION FOR REPEATING PATTERN OF YOSHIMURA (REF. 23) DEFLECTION SHAPE (DASHED LINES EDGES OF TYPICAL TRIANGLES)

"The aeronautical and space activities of the United States shall be conducted so as to contribute . . . to the expansion of human knowledge of phenomena in the atmosphere and space. The Administration shall provide for the widest practicable and appropriate dissemination of information concerning its activities and the results thereof."

—NATIONAL AERONAUTICS AND SPACE ACT OF 1958

NASA SCIENTIFIC AND TECHNICAL PUBLICATIONS

TECHNICAL REPORTS: Scientific and technical information considered important, complete, and a lasting contribution to existing knowledge.

TECHNICAL NOTES: Information less broad in scope but nevertheless of importance as a contribution to existing knowledge.

TECHNICAL MEMORANDUMS: Information receiving limited distribution because of preliminary data, security classification, or other reasons.

CONTRACTOR REPORTS: Technical information generated in connection with a NASA contract or grant and released under NASA auspices.

TECHNICAL TRANSLATIONS: Information published in a foreign language considered to merit NASA distribution in English.

TECHNICAL REPRINTS: Information derived from NASA activities and initially published in the form of journal articles.

SPECIAL PUBLICATIONS: Information derived from or of value to NASA activities but not necessarily reporting the results of individual NASA-programmed scientific efforts. Publications include conference proceedings, monographs, data compilations, handbooks, sourcebooks, and special bibliographies.

Details on the availability of these publications may be obtained from:

SCIENTIFIC AND TECHNICAL INFORMATION DIVISION

NATIONAL AERONAUTICS AND SPACE ADMINISTRATION

Washington, D.C. 20546